Spindle Oscillations are Generated in the Dorsal Thalamus and Modulated by the Thalamic Reticular Nucleus

Chun-Hua Liu[1,2], Yi Ping Guo[1], Xian-Kai Meng[3], Yan-Qin Yu[1,4], Ying Xiong[1,2], Li-Xia Gao[2], Ying-Shing Chan[5], Jufang He[1,2,3*]

[1]Department of Rehabilitation Sciences, The Hong Kong Polytechnic University, Hung Hom, Kowloon, Hong Kong, China
[2]Institute of Neuroscience, Shanghai Institute of Biological Sciences, Chinese Academy of Sciences, Yueyang Rd., Shanghai, China
[3]Nationa Key Laboratory of Brain and Cognitive Sciences, Institute of Biophysics, Chinese Academy of Sciences, Datun Rd., Beijing, China
[4]Department of Physiology, Faculty of Medicine, Zhejiang University, Hangzhou, China
[5]Department of Physiology and Research Centre of Heart, Brain, Hormone and Healthy Aging, LKS Faculty of Medicine, The University of Hong Kong, 21 Sassoon Road, Hong Kong, China

*Correspondence to: Jufang He, Department of Rehabilitation Sciences, The Hong Kong Polytechnic University, Hung Hom, Kowloon, Hong Kong. Tel: +852 2766 6741; Fax: +852 2330 8656, E-mail: rsjufang@polyu.edu.hk

Abbreviated title: Genesis of Spindle Waves

Text pages: 28 pages

Figures: 5

Supplementary materials: 7 Supplementary Figures. Supplementary text, 2 pages

Key words: Sleep spindle; medial geniculate body (MGB); thalamic reticular nucleus (TRN); auditory cortex; posteriopontine tegmentum; electrical stimulation; excitatory postsynaptic potential (EPSP); inhibitory postsynaptic potential (IPSP); GABA receptor antagonist

ABSTRACT

Spindle waves occur during the early stage of slow wave sleep and are thought to arise in the thalamic reticular nucleus (TRN), causing inhibitory postsynaptic potential spindle-like oscillations in the dorsal thalamus that are propagated to the cortex. We have found that thalamocortical neurons exhibit membrane oscillations that have spindle frequencies, consist of excitatory postsynaptic potentials, and co-occur with electroencephalographic spindles. TRN lesioning prolonged oscillations in the medial geniculate body (MGB) and auditory cortex (AC). Injection of $GABA_A$ antagonist into the MGB decreased oscillation frequency, while injection of $GABA_B$ antagonist increased spindle oscillations in the MGB and cortex. Thus, spindles originate in the dorsal thalamus and TRN inhibitory inputs modulate this process, with fast inhibition facilitating the internal frequency and slow inhibition limiting spindle occurrence.

Spindle oscillations occur during the early stage of slow wave sleep and switch the thalamus from its relay function to OFF mode, partially isolating the cortex from sensory inputs and "calming" it. Spindle oscillations consist of 7 – 14 Hz waves that last 1 – 3 s and recur every 5 – 10 s[1-2]. Decades ago, the mechanisms underlying spindle oscillations were proposed to reside in the thalamus[3-4]. In the past twenty-some years, spindle oscillations have been shown in neurons in the ventroanterior-ventrolateral and ventroposterolateral nuclei, dorsal lateral geniculate body, the medial geniculate body (MGB), and reticular nucleus of the thalamus (TRN), *in vivo* and in slice preparations[5-9]. Previous intracellular recordings, performed mainly in deafferented brains, have shown that spindle oscillations in thalamocortical neurons are initiated by a series of inhibitory postsynaptic potential (IPSPs) that are associated with excitatory postsynaptic potentials (EPSPs) in the TRN[5,10]. Moreover, an isolated part of the TRN has been shown to generate spindling rhythmicity[11]. It has previously been thought that TRN cells generate rhythmic (7 – 14 Hz) spike-bursts superimposed on a depolarizing envelope, whereas thalamocortical cells fire rebound bursts when the IPSPs imposed by TRN cells are hyperpolarized enough[12] to remove inactivation of the low-threshold Ca^{2+} spike (LTS)[13]. The spindle rhythmic oscillation is then forwarded to the cortex via the thalamocortical cells. The above notion is supported by slice experiments showing that GABA receptors participate in spindle genesis[6]. A recent study demonstrated that prolonged hyperpolarizing potentials precede spindle oscillations in the TRN[14]. This supports the idea that spindles are initiated in the TRN, which is thought to be the pacemaker of thalamocortical oscillations[8].

We have found that, in the guinea pig, many neurons in the MGB, in which interneurons account for < 1% of the population[15], have spindle oscillations corresponding to EPSPs rather than IPSPs. This phenomenon cannot be explained by our existing knowledge. This, taken with an earlier finding that spindles are present in mice lacking a T-type calcium channel subunit[16], prompted us to further investigate the mechanism of the spindle genesis. To do this, we simultaneously recorded from the MGB, TRN, and cortex following application of $GABA_A$ and/or $GABA_B$ receptor antagonists to the MGB. We minimized the potential involvement of the cortex in spindle genesis by performing *in vivo* intracellular and extracellular recordings in the MGB after ablation or deactivation of the auditory cortex (AC). We also explored possible brainstem modulation of the spindle oscillation in the thalamus through electrical stimulation and/or simultaneous recording.

RESULTS

The results were derived from 42 intracellularly recorded neurons and 75 extracellularly recordings in 70 guinea pigs.

Absence of a direct linkage between thalamic IPSP waves and spindles. Sixteen neurons in the auditory thalamus showed IPSP membrane oscillations with a spindle frequency of 7 – 14 Hz. Electroencephalograms (EEG) in the AC obtained simultaneously with recordings of intracellular membrane potential revealed that only four IPSP spindles co-occurred with EEG spindle waves. However, none of the IPSP spindles were synchronized with the EEG in the AC. The occurrence frequencies differed between EEG and IPSP spindles (0.125 ± 0.007 Hz vs. 0.071 ± 0.004 Hz, respectively, $P < 0.05$), as did the duration (5.01 ± 0.24 s vs. 2.50 ± 0.07 s, respectively $P < 0.05$; n = 4). In the other 12 MGB neurons, IPSP spindles co-occurred with EEG slow-wave oscillations (delta oscillation, Supplementary Fig. 1 and text). The mean occurrence and duration of the IPSP spindles were 0.16 ± 0.02 Hz and 3.44 ± 0.48 s, respectively (n = 12).

Correlation of thalamic EPSP waves with spindles. Twenty-six MGB neurons showed EPSP membrane oscillations that coexisted with EEG spindles recorded in the cortex. All successfully-labeled MGB neurons (n = 7) after intracellular recordings were thalamocortical neurons. Although the synchronization of the EPSP spindles and the EEG spindles was observed in only one case (1/26), the spindles had a similar occurrence frequency (0.122 ± 0.008 Hz for EPSP and 0.134 ± 0.009 Hz for EEG, $P = 0.17$; n = 26) and duration (3.36 ± 0.27 s for EPSP and 3.12 ± 0.18 s for EEG, $P = 0.23$; n = 26). Fig. 1

shows an example of simultaneous EEG recordings in the AC and membrane potential recordings in the thalamocortical neurons of the MGB. The membrane oscillation and burst firings of the MGB neuron in Fig. 1a were not synchronized with the EEG spindle waves (it was very rare to record synchronized spindles in the MGB and AC, one example is shown in Supplementary Fig. 2). For the MGB neuron shown in Fig. 1a, the frequency of the membrane oscillation within a spindle wave was about 7.35 Hz, the same as the frequency in the EEG spindle (see the spectral analyses shown to the right in the middle row of Fig. 1a). The mean frequency of the ESPS spindles was 7.96 ± 1.09 Hz, which is similar to that for EEG spindle waves (8.05 ± 0.96 Hz, P =0.38; n = 26; see population data in Fig. 1b). EEG spindles were synchronized with burst firings detected in the AC through multichannel extracellular recordings (Supplementary Fig. 3).

Figure 1 near here

Effect of $GABA_A$ antagonist injection into the MGB on spindle frequency. The waxing and waning pattern of the MGB spindle oscillation was not altered by application of the $GABA_A$ receptor antagonist, bicuculline (BIM), to the MGB. However, the inter-burst frequency in the MGB spindle oscillations decreased from 7.32 Hz to 4.39 Hz. In addition, the frequency of the spindle waves in the AC decreased from 7.56 Hz to 4.67 Hz (Fig. 2, a and b). The frequency of the MGB spindle oscillation recovered to 7.50 ± 0.43 Hz at 50 min after drug application (Fig. 2c). The time-dependent effects of BIM on the inter-burst frequency, duration, and occurrence frequency of the spindle oscillations are shown in Fig. 2d. The duration of the spindle decreased slightly after drug application, while the occurrence of the spindle increased at 10 min after the drug

application. Population data show that both of the shorting of duration and increasing of occurrence were statistically significant at 30 min after drug application (Fig. 2f).

Changes in the oscillatory frequency within a spindle were analyzed further by comparing the sustained and refractory periods of the bursts in the spindle (see upper row of Fig. 2e). BIM injection significantly lengthened both the sustained (from 72.41 ± 8.55 ms to 102.31 ± 5.99 ms) and refractory period (from 80.54 ± 8.65 ms to 140.41 ± 15.68 ms) within 3 min (Fig. 2e, lower row), and each recovered to pre-injection levels 50 min later.

Figure 2 near here

Effect of $GABA_B$ antagonist injection into the MGB on spindle occurrence and frequency. The inter-burst frequency within spindle oscillations in the MGB and cortex did not change (from 8.49 ± 0.85 Hz to 8.27 ± 0.89 Hz, $P = 0.27$; n = 10) after application of the $GABA_B$ receptor antagonist, CGP35348, to the MGB (Fig. 3a). However, the occurrence of the spindle oscillations was increased from 0.085 ± 0.011 Hz to 0.115 ± 0.010 Hz ($P < 0.001$; n = 10) at 10 min after the drug application.

Figure 3 near here

Effect of combined injection of $GABA_A$ and $GABA_B$ antagonists into the MGB on spindle oscillations. The inter-burst frequency within spindle oscillation was lowered from 7.57 Hz to 5.08 Hz at 10 min after the injection of a combination of BIM and CGP35348 (Fig. 3b), and it returned to 7.43 Hz at 50 min after injection. The antagonists led to the appearance of oscillations that were often sustained for over 10 s. In contrast, the duration of the spindle oscillation was 3.34 s before injection and 3.93 s at 50 min

after injection. The injection of the antagonist mixture into the MGB also affected the frequency of the spindle oscillation in TRN neurons (see TRN1 trace in Fig. 3b).

Effect of TRN lesions on oscillation frequency in the MGB and AC. Two days after the auditory sector of the TRN was lesioned with kainic acid (see Nissl staining of the lesioned TRN in the lower panel of Fig. 3c), oscillations were still present in the MGB and AC. However, in both, the frequency of oscillations was decreased (4.13 ± 0.63 Hz, $P < 0.001$; n = 10), when compared to oscillation frequencies in other cortical fields (10.61 ± 0.75 Hz; Fig. 3c). Lesion of the auditory sector of the TRN produced an effect similar to that resulting from combined application of $GABA_A$ and $GABA_B$ receptor antagonists to the MGB.

Synchronization of spindles and brainstem firings. Synchronization between the EEG spindles of 8.51 ± 0.85 Hz and the laterodorsal tegmental nucleus (LDT)/pedunculopontine tegmental area (PPT) burst firings was detected in 13 animals (an example is shown in Fig. 4a). The burst firings of LDT/PPT neurons appeared earlier than the spindle waves in the cortex (Fig. 4a, lower row). The mean lag time between cortical and LDT/PPT burst firing was 377.1 ± 23.6 ms (13 pairs of recorded sites).

Figure 4 near here

Electrical stimulation of the LDT/PPT triggered oscillatory neuronal activities in the thalamus and cortex that were within the spindle frequency (see example in Fig. 4b). Extracellular recordings of neuronal activities were similar in the AC and MGB. The oscillations lasted from 2.15 to 2.77 s, and differed between recording channels.

Similar to spontaneous spindles, brainstem-triggered oscillations in both the AC and MGB exhibited decreased frequency after application of BIM to the MGB (Fig. 4c). The slowing of the oscillation occurred at about 2 min after the injection in the MGB and 4 min after injection in the AC (Supplementary Fig. 4).

After application of CGP35348 to the MGB (Fig. 4d), the frequency of the brainstem-triggered spindle oscillation remained unchanged (10.45 Hz), but was followed by a different rhythmic activity at 4.25 Hz. This separate rhythmic activity was not observed in the TRN. The frequency of the brainstem-triggered oscillations (4.68 ± 0.37 Hz) was similar to that of the spontaneous oscillation following TRN lesion (4.13 ± 0.63 Hz; Fig. 4e).

Effect of AC ablation on thalamic spindles. EPSP spindle oscillations were observed in the MGB thalamocortical neuron (labeled neuron, Fig. 5a) after the AC was bilaterally ablated. The spindle oscillation, which recurred every 5 –10 s, had a frequency of 8.72 Hz. Reversible inactivation of the AC with lidocaine also did not alter the spindle oscillation in the MGB (Fig. 5b; see Supplementary Fig. 5 for the simultaneous recording of the AC, MGB, and motor cortex before and after lidocaine injection). Indeed, the MGB spindle oscillation had a frequency of 8.40 Hz, which was similar to the 8.53-Hz frequency seen in the motor cortex oscillations.

Figure 5 near here

DISCUSSION

Using *in vivo* intracellular and extracellular preparations, we have demonstrated that the auditory thalamus exhibits spindle-like oscillations. We confirmed the morphologies and locations of some these neurons following intracellular recording experiments, which revealed that 16 of 42 neurons showed a spindle-like oscillation that started with an IPSP, as previously described (*5-6*). The IPSP oscillation was not correlated with the EEG spindle in terms of co-occurrence, and occurrence frequency and duration, while the majority of neurons (26/42) showed spindles that started with and consisted of EPSPs in the MGB with similar occurrence frequency and duration of the oscillation to those of the EEG spindle oscillation. This result indicates that the EEG spindle is correlated with EPSP spindles in the thalamus.

Multiple studies performed within past three decades[5-6,10,17-23] support the notion that TRN cells generate rhythmic (7 – 14 Hz) spike-bursts spindle oscillation and that thalamocortical cells respond to TRN spindle with IPSPs leading to activation of LTS spikes[12,13]. However, this cannot explain the presence of EPSP spindles in MGB neurons or why spindle oscillations are present in the mice lacking a subunit of T-type calcium channels[16], which are supposedly responsible for LTS spikes in the dorsal thalamus.

In contrast to prolonged spike/spike-train sequences (> 1s) on the EPSP spindles in the present study (Fig. 1), a shortfall in the previous recordings was failing to show a full sequence of LTS bursts in spindle frequency at the thalamocortical neurons[1,6,24,25]. With only IPSP oscillation and no spike/spike-train sequence, the thalamocortical neuron was unable to relay the oscillation to the cortex.

Our result that injection of a combination of $GABA_A$ and $GABA_B$ antagonists into the MGB or TRN lesion resulted in slowed oscillation in the MGB reflected that dorsal thalamus could generate the rhythmic oscillation independently at 4 – 5 Hz. This result echoes a recent finding that the thalamocortical neurons could generate synchronized oscillations at 2-13 Hz by themselves under certain depolarized conditions in slice preparations[26].

The waxing and waning pattern of the MGB spindle oscillation did not change in response to application of a $GABA_A$ receptor antagonist. However, application of the $GABA_A$ receptor antagonist to the MGB did block fast inhibitions arising from the TRN, resulting in a slower spindle oscillation (4.39 Hz) in the MGB and AC. The oscillatory burst-firing of the MGB neurons would be expected to trigger responses of TRN neurons, which in turn would inhibit firing of the MGB. This would result in a shortened burst firing and a shortened refractory period until the next burst firing. Thus, feedback inhibition from the TRN on the thalamocortical neurons through $GABA_A$ receptors likely shortens the duration of the burst and inter-burst interval, leading to an oscillation of a higher frequency of 7 – 14 Hz in the dorsal thalamus.

With slice preparation, a slow oscillation of about 3 Hz was observed in both perigeniculate and dorsal lateral geniculate nuclei after BIM perfusion, and was suggested generated through the activation of large, slow $GABA_B$-receptor-mediated IPSPs in the thalamocortical cells by perigeniculate neurons[6]. However, with *in-vivo* preparation, we found that the slowing of spindle oscillation occurred at the MGB before the TRN after BIM injection in the MGB as shown in our multiple electrode recordings

in both TRN and MGB in Supplementary Fig. 6. It is also interesting to note the TRN neurons showed two rhythms in their oscillation at 3 min after BIM injection in MGB, when the MGB has already slowed its oscillation (Supplementary Fig. 6b), indicating that the TRN followed MGB in the shift of oscillatory rhythm. The result shown in Fig. 4d that the MGB showed oscillations of two frequencies (10.45 Hz and 4.25 Hz), while the TRN showed only one frequency of 10.45 Hz would again support that the slower frequency of 4.25 Hz was not related to the TRN. This slow oscillation was likely the same as that observed at the TRN-lesioned MGB, or that observed at the MGB with both GABA antagonists injection.

The inter-burst frequency within the spindle oscillation in the MGB and cortex was not altered by application of a $GABA_B$ receptor antagonist to the MGB. However, the occurrence of the spindle oscillations was increased after the drug application. Feedback inhibition through $GABA_B$ receptors may suppress the occurrence frequency of spindle oscillation by adjusting the resting membrane potential of the thalamocortical cells. In the presence of $GABA_B$ receptor antagonist, the rapid and dynamic inhibition from the TRN to the MGB was retained, because the $GABA_A$ receptors were intact. The TRN neurons have a fast adaptation after the each spindle epoch (X.J. Yu, X.X. Xu, X. Chen, S.G. He, J. He: unpublished observation: Initial exposure to repeated auditory stimuli elicited strong responses from TRN neurons; however, weaker responses were observed in the subsequent trials. This adaptation disappeared when the ISI exceeded 3

s.). This may account for our observation that the spindle oscillations were followed by oscillations with a lower frequency of 4.25 Hz in the MGB (Fig 4D).

The question arises as to why, over the past 24 years, investigators have not detected spindles in thalamocortical neurons that were initiated by and consisted of EPSPs. This is probably due the differences in the experimental preparation. Most intracellular recording studies have been carried out with slice preparations or deafferented brain preparations[5,6,10,20,22-23]. Deschênes and colleagues reported the presence of EPSP spindles in the ventral lateral nucleus but concluded that they were from thalamic interneurons (*5*). In *cerveau isolé* preparations or slice preparations, the projections from the brainstem reticular activation system to the forebrain, which are the major source of neurotransmitters such as acetylcholine, norepinephrine, and serotonin, are disconnected[27-30]. When a neuron is hyperpolarized to between -65 mV and -72 mV, the excitatory inputs become less effective, and inhibitory inputs decrease the membrane potential even further, causing LTS spikes[31-33]. In the absence of a major excitatory input from the brainstem activation system (the LDT/PPT), the thalamocortical neurons are likely placed in a hyperpolarized state, and inhibitory inputs from the TRN cause further hyperpolarization, resulting in spindle-like IPSPs with LTS spikes.

Here, analysis of an intact nervous system with simultaneous recording from the LDT/PPT and cortex showed that the spindle wave in the cortex was synchronized with and preceded by the LDT/PPT burst firing for hundreds of milliseconds (Fig. 4). Electrical stimulation of the LDT/PPT triggered EEG oscillation and burst firing in the MGB, with both being within the spindle frequency (Fig. 4). Recent studies by Hughes

and colleagues showed that activation of the metabotropic glutamate receptor can cause synchronized oscillations at α and θ frequencies (2 – 15 Hz) with high-threshold burst firings[26,34]. The periodic activity of LDT/PPT neurons would provide periodic release of acetylcholine or glutamate in the thalamus and/or cortex[35-36] and may trigger the spindle oscillation in the thalamus and cortex. Consistent with this idea, brainstem peribrachial stimulation alters spindle oscillations in the TRN[22].

Concluding Remarks

The discovery of EPSP spindles in the thalamocortical neurons rejects the notion that spindle waves are generated in the TRN and forwarded to the cortex through LTS bursts, which result from IPSP spindles in the thalamocortical neurons. Our results show that the spindle oscillation is generated between the dorsal thalamus and the TRN. Indeed, the dorsal thalamus could generate a low-frequency (4.13 Hz) and long-lasting oscillation by itself. The feedback inhibition from the TRN on the thalamocortical neurons through $GABA_A$ receptors shortened the duration of the burst and inter-burst-interval, facilitated the inter-burst frequency to 7 – 14 Hz in the dorsal thalamus. The feedback inhibition through $GABA_B$ receptors suppressed the occurrence frequency of spindle oscillation. Taken together, our results support the idea that the spindle is triggered/managed by the PPT/LDT, generated in the dorsal thalamus, modulated by the TRN, and propagated to the forebrain.

MATERAILS AND METHODS

Surgical preparation of animals

Anesthesia was initially induced with pentobarbital sodium (Nembutal, Abott, 35 mg/kg, i.p.) and maintained by supplemental doses of the same anesthetic (about 5 – 10 mg/kg/hr) during the surgical preparation and recording. Throughout the recording, the EEG was monitored to assess the level of anesthesia. Following induction of anesthesia, guinea pigs were mounted in a stereotaxic device with hollow ear bars. A midline incision was made in the scalp and craniotomies were performed to enable vertical access to the medial geniculate body (MGB), the the laterodorsal tegmental nucleus (LDT)/pedunculopontine tegmental area (PPT), and/or the thalamic reticular nucleus (TRN) in the right hemisphere[31,36]. The experimental procedures were approved by the Animal Subjects Ethics Committees of Hong Kong Polytechnic University and Institute of Neuroscience, Chinese Academy of Sciences.

Intracellular recording

For intracellular recording, cerebrospinal fluid was released at the medulla level through an opening at the back of the neck. The animal was artificially ventilated. Both sides of the animal's chest were opened, and its body was suspended to reduce vibrations to the brain caused by intra-thoracic pressure.

The auditory thalamus was targeted for intracellular recording. We used a glass pipette as the recording electrode, filling it with either 1.0 M KCl or 3.0 M KAc (pH 7.6). The resistance of the electrode ranged between 40 – 90 MΩ. The electrode was advanced vertically from the top of the brain by a stepping motor (Narishige, Tokyo, Japan). After the electrode was lowered to a depth of 4 – 5 mm, the cortical exposure was sealed using

low-melting temperature paraffin. When the electrode was near or in the target area, it was slowly advanced at 1 or 2 μm per step. A low impedance electrode was placed under the scalp at either the auditory cortex or the frontal lobe to record the EEG.

In ten experiments, an additional metal electrode was implanted in the auditory sector of the TRN. In these experiments, activities of TRN neurons were simultaneously recorded with those of MGB and LDT/PPT neurons, along with EEG activity.

In 15 experiments, 2 or 3 metal electrodes of 1 – 3 MΩ were implanted in the brainstem, targeting the PPT and LDT. Neuronal activities of single/multiple units were recorded through the metal electrodes. Along with the recording electrodes, three parallel low-stimulation electrodes were implanted into the brainstem targeting the LDT/PPT areas. In most cases, we applied 1 – 5 electrical current pulse trains with a 0.5-ms width and a 50-Hz frequency to activate the LDT/PPT[37]. Electrical currents of 50 – 200 μA were applied to the brainstem, ipsilateral to the recording thalamus. Neuronal responses in the MGB, TRN, and auditory cortex to the electrical stimulation of the LDT/PPT were simultaneously recorded. To eliminate the possibility of the involvement of the cortex in the genesis of spindle oscillation, we ablated the auditory cortex (5.0×4.0 mm^2) with a suction pump (REFCO, ROYAL-2) in four animals.

Extracellular recording

Thirty extracellular recording experiments were performed. A six-electrode array with an inter-electrode space of 200 μm and a resistance of 3 – 4 MΩ was inserted into the MGB. A four-electrode array with 3 – 4 MΩ resistance was implanted in the TRN, and a six-electrode array of mixed high and low impedance was implanted in the auditory

cortex. A stimulation electrode array of low impedance was implanted in the LDT/PPT. The electrical stimulation paradigm was the same as that used for the intracellular preparation. Simultaneous recordings were carried out from the electrode arrays in different parts of the brain during spontaneous firing, in response to acoustic stimuli, or following electrical activation of the LDT/PPT.

In ten experiments, the TRN was lesioned by injection of kainic acid (KA, Tocris, 2.5g/L in 0.9% saline solution, 0.3 μl). Recordings in the MGB and auditory cortex neurons were performed 2 – 3 days after lesioning, when maximum loss of cell bodies occurred[38,39]. The extent of TRN lesions was determined on Nissl-stained coronal sections of 90 μm thickness.

In thirty experiments, the recording electrode array in the MGB was combined with a glass pipette filled with $GABA_A$ antagonist (BIM, 15 mM, 0.1 μl), $GABA_B$ antagonist (CGP35348, 20 mM, 0.1 μl), or a combination of these compounds. A Hamilton syringe connected to a 40 μm-diameter glass pipette was used for microinjection.

In five experiments, the auditory cortex was reversibally inactivated by injection of lidocaine (20 mg/ml, 1 μl). The implanted electrode arrays were used to simultaneously record neural activities in the different areas.

Anatomical confirmation

The glass pipette used for intracellular recording was filled with neurobiotin (Neurobiotin™, Vector, 1 – 2% in 1.0 M KCl and 3.0 M KAc), and the tracer was injected into 1 or 2 neurons of each subject after physiological recordings of the eight

subjects were complete. Neurobiotin was delivered into the neuron by applying rectangular depolarizing current pulses (150 ms, 3.3 Hz, 2 nA) for 1 – 4 min.

To confirm that the recording/stimulation electrodes were located in the PPT/LDT, we applied electrical current through the recording/stimulation electrode to make a lesion in the brainstem. Analysis of Nissl-stained tissue revealed that, in seven subjects, the recording/stimulation electrodes were properly positioned in the PPT/LDT. Chemical lesion of the TRN was confirmed with Nissl staining. Histological processing was performed as previously described[40,41].

Data acquisition and analysis

In intracellular recording, the electrode detected the negative membrane potential upon penetrating the membrane of a cell. After amplification, the membrane potential of the MGB neuron as well as the EEG and the extracellular signals of LDT/PPT and TRN neurons were stored in the computer with the aid of commercial software (AxoScope, Axon). The direct current level of the recording electrode was frequently checked and set to zero during the course of the experiments. The direct current level after each recording was used to compensate for the membrane potential of some neurons, especially for those with a long recording time. Only those neurons showing a resting membrane potential lower than –50 mV and spontaneous spikes (if any) greater than 50 mV were included in the study.

The occurrence frequency and duration of IPSP and EPSP spindle-like oscillations, as well as EEG spindles were averaged over ten consecutive trials for each neuron. The frequency of the EPSP oscillation was calculated using the fast-fourier

transform algorithm (FFT). The time lag between the PPT burst firing and EEG spindle was averaged over five consecutive trials for each case.

For extracellular recordings, the frequencies of rhythmic activities were calculated using FFT, based on the envelope of the neural activities. The sustaining of the burst firing of the neurons was calculated based on the time between the two points of the baseline was doubled, while the refractory period was the remainder of the rhythmic cycle. The ANOVA or Student's t-test was used for the comparisons. $P < 0.05$ was considered significant.

REFERENCES AND NOTES

1. Steriade, M. & Deschênes, M. The thalamus as a neuronal oscillator. *Brain Res. Rev.* **8**, 1-63 (1984).
2. Steriade, M. Spindling, incremental thalamocortical responses, and spike-wave epilepsy. In Generalized Epilepsy (eds Avoli M, Gloor P, Kostopoulos G and Naquet R), pp 161-180. Birkhaüser, Boston (1990).
3. Morizon, R. S. & Bassett, D. L. Electrical activity of the thalamus and basal ganglion in decorticate cats. *J. Neurophysiol.* **8**, 309-314 (1945).
4. Andersen, P. & Andersson, S. A. Physiological Basis of the Alpha Rhythm. Appleton-Century-Crofts, New York (1968).
5. Deschênes, M. Paradis, M., Roy, J. P. & Steriade, M. Electrophysiology of neurons of lateral thalamic nuclei in cat: resting properties and burst discharges. *J. Neurophysiol.* **51**, 1196-1219 (1984).
6. Kim, U., Sanchez-Vives, M.V. & McCormick, D.A. Functional dynamics of GABAergic inhibition in the thalamus. *Science* **278**, 130-134 (1997).
7. Golshani, P., & Jones, E. G. Synchronized paroxysmal activity in the developing thalamocortical network mediated by corticothalamic projections and “silent” synapses. *J. Neurosci.* **19**, 2865-2875 (1999).
8. Fuentealba, P. & Steriade, M. The reticular nucleus revisited: Intrinsic and network properties of a thalamic pacemaker. *Prog. Neurobiol.* **75**, 125-141 (2005).
9. He, J. Slow oscillation in non-lemniscal auditoru thalamus. *J. Neurosci.***23**, 8281-8290 (2003).

10. Steriade, M., Deschênes, M., Domich, L. & Mulle, C. Abolition of the spindle oscillations in thalamic neurons disconnected from nucleus reticularis thalami. *J. Neurophysiol.* **54**, 1473-1497 (1985).
11. Steriade, M., Domich, L., Oakson, G. & Deschênes, M. The deafferented reticularis thalami nucleus generates spindle rhythmicity. *J. Neurophysiol.* **57**, 260-273 (1987).
12. Steriade, M. & Deschênes, M. Intrathalamic and brain stem-thalamic networks involved in resting and alert states. In: Cellular Thalamic Mechanisms (eds Bentivolglio M and Spreafico R) pp 51-76. Elsevier, Amsterdam (1988).
13. Johnsen, H. & Llinás, R. R. Ionic basis of electroresponsiveness and oscillatory properties of guinea pig thalamic neurones in vitro. *J. Physiol. (Lond.)* **349**, 227-247 (1984).
14. Fuentealba, P., Timofeev, I. & Steriade, M. Prolonged hyperpolarizing potentials precede spindle oscillations in the thalamic reticular nucleus. *Proc. Natl. Acad. Sci. USA* **101**, 9816-9821 (2004).
15. Arcelli, P., Frassoni, C., Regondi, M. C., De Biasi, S., & Spreafico, R. GABAergic neurons in mammalian thalamus: A marker of complexity? *Brain Res. Bull.* **42**, 27-37 (1997).
16. Lee, J., Kim, D. & Shin, H.S. Lack of delta waves and sleep disturbances during non-rapid eye movement sleep in mice lacking a1G-subunit of T-type calcium channels. *Proc. Natl. Acad. Sci. USA* **101**,18195-18199 (2004).
17. Contreras, D. & Steriade, M. Cellular basis of EEG slow rhythms: a study of dynamic corticothalamic relationships. *J. Neurosci.* **15**, 604-622 (1995).

18. Contreras, D. & Steriade, M. Spindle oscillation in cats: the role of corticothalamic feedback in a thalamically generated rhythm. *J. Physiol. (Lond.)* **490**, 159-179 (1996).

19. Steriade, M. Neocortical cell classes are flexible entities. *Nat. Rev. Neurosci.* **5**, 121-134 (2004).

20. Steriade, M., Jones, E. G. & McCormick, D. A. Thalamus: Organization and Function (vol. 1). Amsterdam: Elsevier Science (1997).

21. Mulle, C., Madariaga, A. & Deschênes, M. Morphology and electrophysiological properties of reticularis thalami neurons in cat: in vivo study of a thalamic pacemaker. *J. Neurosci.* **6**, 2134-2145 (1986).

22. Hu, B., Steriade, M. & Deschênes, M. The effects of brainstem peribrachial stimulation on perigeniculate neurons: The blockage of spindle waves. *Neuroscience* **31**, 1-12 (1989).

23. Destrxhe, A., McCormick, D. A. & Sejnowski, T. J. A model for 8-10 Hz spindling in interconnected thalamic relay and reticularis neurons. *Biophys. J.* **65**, 2474-2478 (1993).

24. Bal, T., von Krosigk, M. & McCormick, D. A. Role of the ferret perigeniculate nucleus in the generation of synchronized oscillations in vitro. *J. Physiol. (Lond.)* **483**, 665-685 (1995).

25. Timofeev, I., Bazhenov, M., Sejnowski, T.J. & Steriade, M. Contribution of intrinsic and synaptic factors in the desynchronization of thalamic oscillatory activity. *Thal. Rel. Syst.* **1**, 53-69 (2001).

26. Hughes, S.W., Lörincz, M., Cope, D.W., Blethyn, K.L., Kékesi, K.A., Parri, H.R., Juhász, G.& Crunelli, V. Synchronized oscillations at α and θ frequencies in the lateral geniculate nucleus. *Neuron* **42**, 253-268 (2004).
27. Moruzzi, G. & Magoun, H.W. Brain stem reticular formation and activation of the EEG. *Electroencephalogr. Clin. Neurophysiol.* **1**, 455-473 (1949).
28. Scheibel, M.E. & Scheibel, A.B. Structural substrates for integrative patterns in the brain stem reticular core. In: Reticular Formation of the Brain (Henry ford Hospital International Symposium) (eds Jasper HH, Proctor LD et al.) pp. 31-55. Little, Brown, Boston (1958).
29. Fitzpatrick, D., Diamond, I.T. & Raczkowski, D. Cholinergic and monoaminergic innervation of the cat's thalamus: Comparison of the lateral geniculate nucleus with other principal sensory nuclei. *J. Comp. Neurol.* **288**, 647-675 (1989).
30. Steriade, M., Paré, D., Parent, A. &mith, A. Projections of cholinergic and non-cholinergic neurons of the brainstem core to relay and associational thalamic nuclei in the cat and macaque monkey. *Neuroscience* **25**, 47-67 (1988).
31. Yu, Y.Q., Xiong, Y., Chan, Y.S. & He, J.F. In vivo intracellular responses of the medial geniculate neurones to acoustic stimuli in anaesthetized guinea pigs. *J. Physiol. (Lond.)* **560**, 191-205 (2004).
32. Xiong, Y., Yu, Y.Q., Chan, Y.S. & He, J.F. Effects of cortical stimulation on auditory-responsive thalamic neurones in anaesthetized guinea pigs. *J. Physiol. (Lond.)* **560**, 207-217 (2004).

33. Yu, Y.Q., Xiong, Y., Chan, Y.S. & He, J.F. Corticofugal gating of auditory information in the thalamus: an in-vivo intracellular recording study. *J. Neurosci.* **24**, 3060-3069 (2004).

34. Hughes, S.W., Cope, D.W., Blethyn, K.L. & Crunelli, V. Cellular mechanisms of the slow (<1 Hz) oscillation in thalamocortical neurons in vitro. *Neuron* **33**, 947-958 (2002).

35. Clements, J.R. & Gant, S.J. Glutamate-like immunoreactivity in neurons of the laterodorsal tegmental and pedunculopontine nuclei in the rat. *Neurosci. Lett.* **120**, 70-73 (1990).

36. Lavoie, B. & Parent, A. Pedunculopontine nucleus in the squirrel monkey: distribution of cholinergic and monoaminergic neurons in the mesopontine tegmentum with evidence for the presence of glutamate in cholinergic neurons. *J. Comp. Neurol.* **344**,190-209 (1994).

37. Steriade, M., Datta, S., Paré, D., Oakson, G. & Curró Dossi, R. Neuronal activities in brain-stem cholinergic nuclei related to tonic activation processes in thalamocortical system. *J. Neurosci.* **10**, 2541-2559(1990).

38. Deschênes, M. & Hu B. Electrophysiology and pharmacology of the corticothalamic input to lateral thalamic nuclei: an intracellular study in the cat. *Eur. J. Neurosci.* **2**, 140-152, (1990).

39. McGeer, E.G., Olney, J.W. & McGeer, P.L. Kainic acid as a tool in neurobiology. New York: Raven Press, 1978, p. xii, 271 p.

40. Guo, Y.P., Sun, X., Li, C., Wang, N.Q., Chan, Y.S. & He, J. Corticothalamic synchronization leads to c-fos expression in the auditory thalamus. *Proc. Natl. Acad. Sci. U.S.A* . **104**, 11802-11807 (2007).

41. Zhang, Z,, Liu, C.H., Yu, Y.Q., Fujimoto, K., Chan, Y.S. & He, J. Corticofugal projection inhibits the auditory thalamus through the thalamic reticular nucleus. *J. Neurophysiol.* **99**, 2938-2945 (2008).

ACKNOWLEDGMENTS: The authors appreciate Shigang He at Institute of Biophysics, Chinese Academy of Sciences for assistance in histological processing of labeled cells. We also thank Simon S.M. Chan and Kimmy F.L. Tsang of The University of Hong Kong for their excellent technical assistance in histological preparations. The study was partially supported by the Hong Kong Research Grants Council (CERG PolyU5373/04M, 5467/05M) and the Institute of Neuroscience, Chinese Academy of Sciences.

FIGURE LEGENDS

Figure 1 Spindle-like EPSP oscillations in thalamocortical neurons and EEG spindles. (**a)** Upper two traces show a simultaneous EEG recording in the AC and intracellular recording from an MGB neuron. A spindle-like EPSP oscillation is shown in the middle row, along with the corresponding EEG. The spectra of the EEG and EPSP spindles, as analyzed by FFT, are shown on the right. The MGB neuron located at the caudal part of the MGB was labeled after recording and is shown in the lower row. Scale bars: 100 μm and 1.0 mm in the left and right panels, respectively. (**b**) Comparison of spindle frequency, duration, and occurrence of spindle waves between cortical spindles and EPSP spindles of the MGB. .

Figure 2 Injection of $GABA_A$ antagonist into the MGB slows spindle oscillations. (**a-c**) Spontaneous spindle oscillation in the MGB and AC before and after BIM injection into the MGB. Two channels of extracellular recordings from the MGB, three channels of field potentials, and one extracellular recording from the AC that were obtained simultaneously are shown. Scale bar: 1 s for all. The envelopes of extracellular recordings, and field potentials, of selected channels of spindle waves were analyzed by FFT. (**d**) Time-dependent effect of BIM injection on the frequency within spindle waves, as well as their duration and occurrence. (**e**) Effect of BIM injection on sustained and refractory periods of oscillatory bursts within the spindle oscillation. (**f**) Population result of time-dependent effect of BIM injection on the frequency within spindle waves, and the duration and occurrence of spindle waves.

Figure 3 Spindle oscillations are modulated by TRN inhibition. (**a**) Spontaneous spindle oscillations in the MGB, TRN, AC, and motor cortex (MC) after injection of the $GABA_B$ antagonist, CGP35348, into the MGB. Scale bar: 1 s for all. The spectra of the envelopes were analyzed over the time epochs indicated by 1 and 2. (**b**) Spontaneous oscillations in the MGB, TRN, and AC after combined injection of BIM and CGP35348 in the MGB. The spectra were analyzed using the envelopes of extracellular recordings of selected channels in the MGB and TRN for the indicated period. (**c**) Spontaneous oscillations in the MGB and AC two days after a chemical lesion of the auditory sector of the ipsilateral TRN. The spectra were analyzed using extracellular recordings of selected channels in the MGB and AC for the indicated period. Photomicrographs show Nissl staining of the control and lesioned TRN.

Figure 4 Spindle oscillations are synchronized with spontaneous firing in the brainstem reticular formation and are triggered by electrical stimulation of the brainstem reticular formation. (a) Synchronization of the EEG spindles and neuronal activities of the brainstem reticular formation in the PPT (See Supplementary Fig. 7 for location). EEGs in the AC were recorded simultaneously with the extracellular neuronal activities in the PPT. The inset shows a spindle wave with synchronized PPT neuronal activity and EEG activity. The spectral analysis of the EEG spindle is shown on the left. (**b-e**) Effect of electrical stimulation (ES) of the PPT on oscillatory activities in the MGB, AC, and TRN. Oscillatory activities were recorded under normal condition (**b**), 10 min after BIM

injection into the MGB (**c**), 10 min after CGP35348 injection into the MGB (**d**), and 2 days after TRN lesion (**e**). The left panel shows the multichannel recordings. The right panel shows spectral analyses of each oscillation epoch in selected channels of the recordings on the left.

Figure 5 MGB spindles are preserved in the absence of a functional cortex. (**a)** The upper trace shows an intracellular recording from an MGB neuron in an animal with a bilaterally ablated AC. An episode of the EPSP spindle is shown in the middle row on the right. The spectral analysis of the membrane oscillation is shown on the left. The recorded MGB neuron was labeled with neurobiotin. Its location and morphology are shown. Scale bar: 1.0 mm. (**b**) Multichannel recording of the MGB and motor cortex following reversible inactivation of the ipsilateral cortex with lidocaine. The frequency of the spindle oscillation in the MGB was unaffected, as shown in the spectral analysis. [multichannel recordings from the MGB, motor cortex, and AC before and after (3 min) AC inactivation are shown in Supplementary Fig. 4].

Supplementary on-line Materials:

1. Supplemenary figures

Supplementary Fig. 1 Spindle-like membrane oscillations in thalamocortical neurons that consist of inhibitory postsynaptic potentials (IPSPs) do not correlate with cortical spindle waves. (**a**) Traces showing simultaneous EEG recordings of the auditory cortex, intracellular recordings of a medial geniculate (MGB) neuron, and extracellular recordings of thalamic reticular nucleus (TRN) neurons. An IPSP wave and synchronized TRN activity are shown, along with the EEG, in the right lower row. The spectrum of IPSP membrane oscillation (shown on the left) was analyzed using fast-Fourier-transform (FFT) analysis with a Hanning window. (**b-c**) Traces showing simultaneous EEG recordings and intracellular recordings of MGB neurons. Traces on the lower row of (**c)** show a depicted IPSP oscillation (right) and its spectral analysis (left). See supporting text for more information.

Supplementary Fig. 2 The EPSP oscillations of the thalamocortical neuron in Fig. 2. This neuron had a frequency of 9.0 Hz and roughly co-occurred with EEG spindle waves in the cortex. Spikes or spike bursts were accompanied by EPSPs. The co-occurrence of the EPSP oscillation with the EEG spindles was easier to detect after the EPSP oscillation was filtered (7 – 14 Hz, second trace).

Supplementary Fig. 3 Rhythmic burst firings with spindle frequency detected with extracellular recordings are synchronized with field potential recordings in the cortex.

Four-channel extracellular recordings and two-channel field potential recordings were obtained from electrodes placed in the AC. Signals from a spindle episode are shown in the lower part of the figure.

Supplementary Fig. 4 Oscillatory frequency within the spindle is slowed by injection of a $GABA_A$ antagonist (BIM) into the MGB. Changes in the oscillatory frequency in the MGB and AC are shown (**a**) before BIM injection and at (**b**) 2 min, (**c**) 4 min, (**d**) 10 min, (**e**) 30 min, and (**f**) 50 min after BIM injection. Spectral analyses of the spindle episodes are shown in the right panel. The oscillatory frequency was slowed in the MGB immediately after the BIM injection, while this effect was more delayed in the AC. By 4 min, both the MGB and AC showed an oscillatory frequency of 4.46 Hz. The frequency started to increase at 10 min (5.51 Hz) and reached pre-injection levels at 50 min (7.41 Hz).

Supplementary Fig. 5. The cortex is not involved in the spindle generation. The spindle oscillation in the MGB was not affected by reversible inactivation of the AC. Multichannel recordings from the AC, MGB, and motor cortex (MC) are shown (**a**) before and (**b**) 3 min after lidocaine injection into the AC. Note that the AC was active before the injection, became inactive at 3 min after the injection, and recovered at 15 min after the injection. The dose of lidocaine applied was sufficient to inactivate the entire AC, as shown by the neuronal activities in the AC (6 electrodes separated by 0.5 mm).

The frequency and the waxing and waning shape of the spindle oscillation in the MGB was unaffected by AC inactivation.

Supplementary Fig. 6. The MGB precedes TRN in slowing of oscillatory frequency after injection of $GABA_A$ antagonist in the MGB. Simultaneous recordings of the MGB and TRN are shown (**a**) before, (**b**) 3 min, (**c**) 20 min, and (**d**) 50 min after BIM injection. Note in (B) that the TRN neurons showed two rhythms in their oscillation at 3 min after BIM injection in MGB, when the MGB has already slowed its oscillation, indicating that the TRN followed MGB in the shift of oscillatory rhythm. The rhythm of oscillations became the same in both MGB and TRN at 20 min after the injection.

Supplementary Fig. 7. Recording or stimulation of the brainstem reticular formation was location at the PPT and LDT. An example shows the location of the recording electrode in the brainstem. IC, inferior colliculus; LL, lateral lemniscus; Pn, pontine nucleus.

2. Supporting text

Absence of a correlation between IPSP oscillations and EEG spindles

Supplementary Fig. 1 shows two examples that the EEG, intracellular recording of MGB neurons, and extracellular recording of TRN neuron (only in Supplementary Fig.1a). Supplementary Fig. 1a shows that the IPSP oscillation of an MGB neuron was synchronized with the firing of TRN neurons, indicating that the IPSPs were likely triggered by TRN inhibition. This result echoes previous findings that, in thalamocortical neurons, IPSPs with spindle frequencies are caused by firing of TRN neurons[1,2]. However, no firings in spindle frequency were detected in the MGB neuron, and no spindle waves were detected in the EEG. Instead, the waves that were detected were in the delta frequency range (1 – 4 Hz) (see EEG in Supplementary Fig. 1a). The neuron shown in Supplementary Fig. 1b showed IPSP oscillations within spindle frequency. The neurons showed LTS spikes during IPSP oscillation; however, no EEG spindle was detected. The neuron in Supplementary Fig. 1c showed IPSP oscillations at about 9 Hz, while the EEG in the AC showed obvious spindle waves. However, the occurrence of the IPSP oscillation and EEG spindles was not synchronized and spindles did not share the same frequency or duration.

4. **References:**

1. M. Deschênes, M.Paradis, J. P. Roy, M. Steriade, Electrophysiology of neurons of lateral thalamic nuclei in cat: resting properties and burst discharges. *J. Neurophysiol.* **51**, 1196-1219 (1984).

2. U. Kim, M.V. Sanchez-Vives, D.A. McCormick, Functional dynamics of GABAergic inhibition in the thalamus. *Science* **278**, 130-134 (1997).

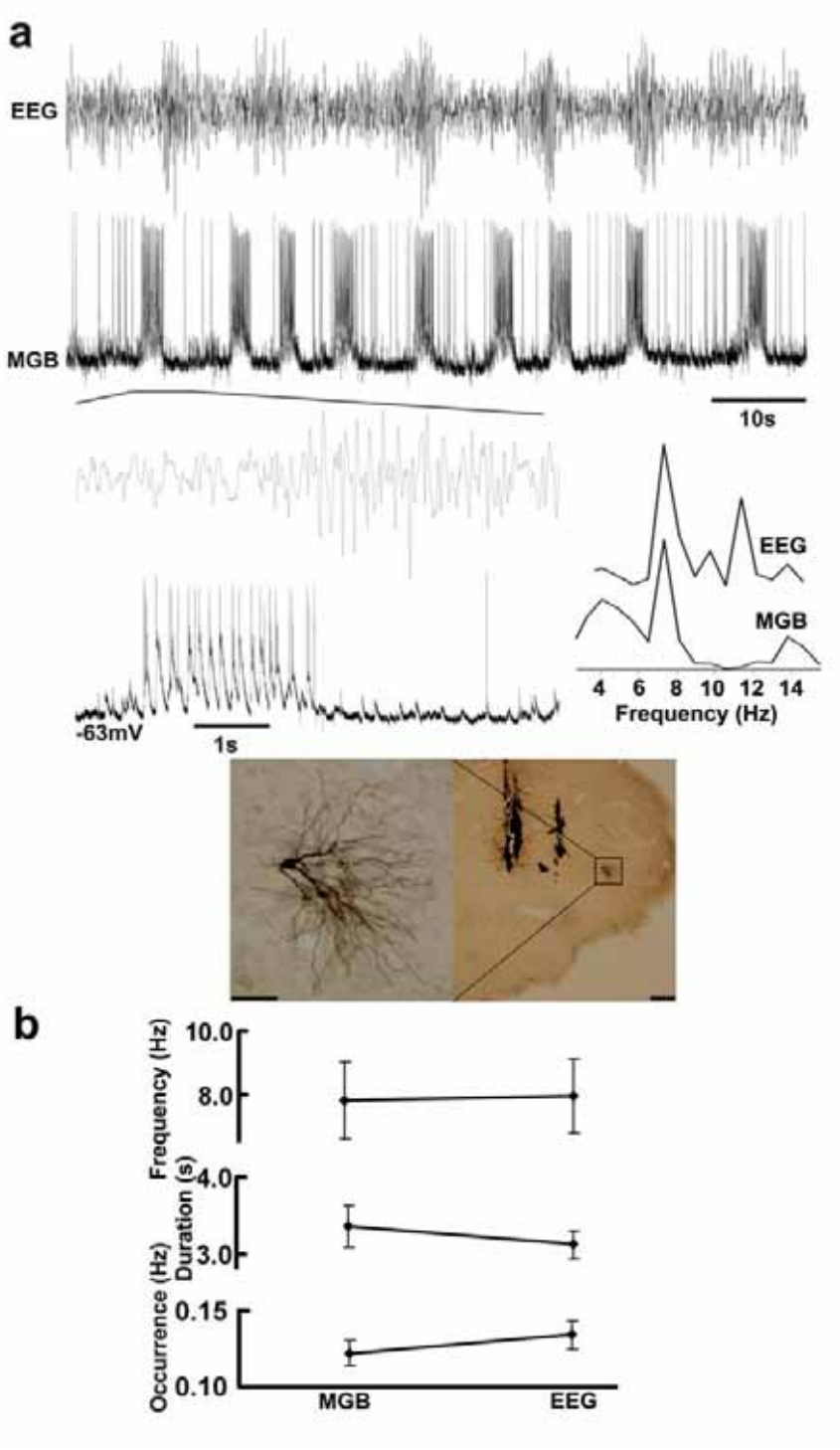
a
EEG
MGB
10s
EEG
MGB
4 6 8 10 12 14
Frequency (Hz)
-63mV
1s
b
Frequency (Hz)
10.0
8.0
Duration (s)
4.0
3.0
Occurrence (Hz)
0.15
0.10
MGB
EEG

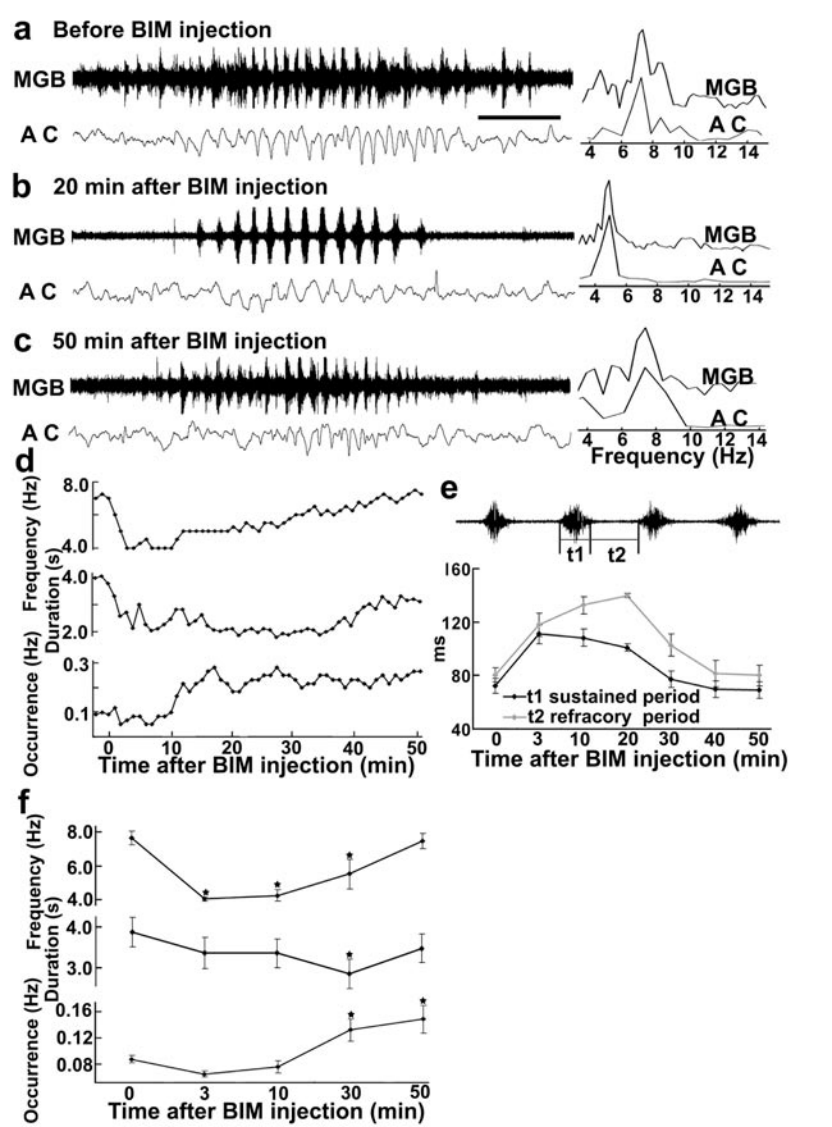
a Before BIM injection
MGB
A C
MGB
A C
4 6 8 10 12 14
b 20 min after BIM injection
MGB
A C
MGB
A C
4 6 8 10 12 14
c 50 min after BIM injection
MGB
A C
MGB
A C
4 6 8 10 12 14
Frequency (Hz)
d
Frequency (Hz)
Duration (s)
Occurrence (Hz)
8.0
4.0
4.0
2.0
0.3
0.1
0 10 20 30 40 50
Time after BIM injection (min)
e
t1
t2
160
120
80
40
ms
t1 sustained period
t2 refracory period
0 3 10 20 30 40 50
Time after BIM injection (min)
f
Frequency (Hz)
Duration (s)
Occurrence (Hz)
8.0
6.0
4.0
4.0
3.0
0.16
0.12
0.08
0 3 10 30 50
Time after BIM injection (min)

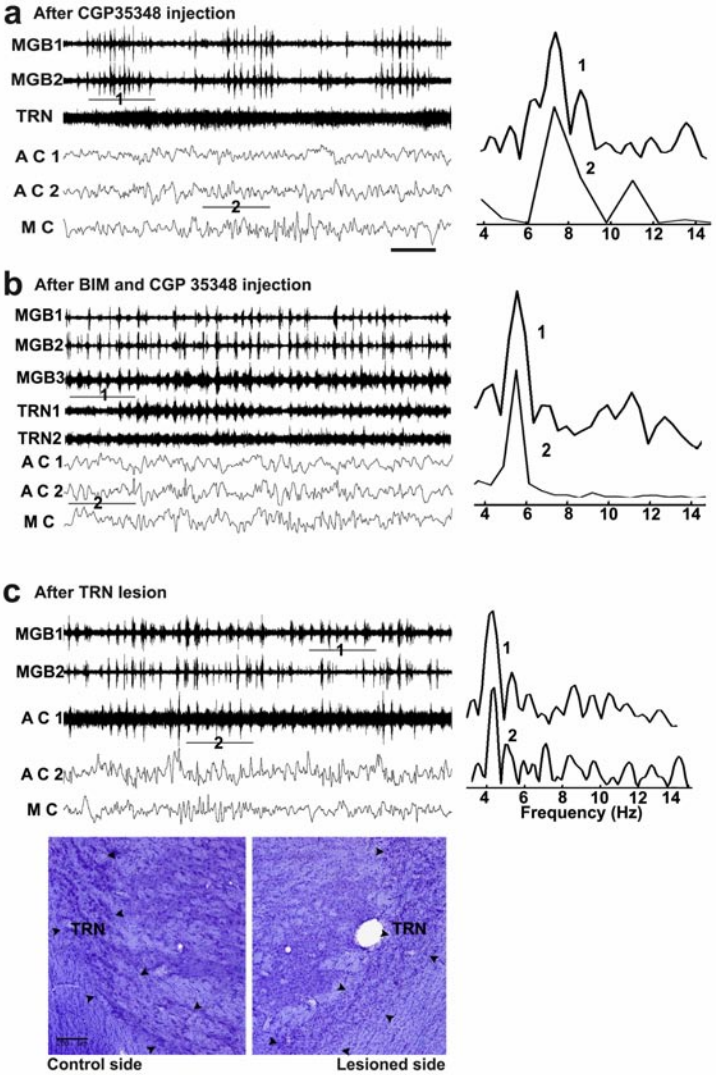
a After CGP35348 injection
MGB1
MGB2
TRN
A C 1
A C 2
M C
1
2
4 6 8 10 12 14
b After BIM and CGP 35348 injection
MGB1
MGB2
MGB3
TRN1
TRN2
A C 1
A C 2
M C
4 6 8 10 12 14
c After TRN lesion
MGB1
MGB2
A C 1
A C 2
M C
4 6 8 10 12 14
Frequency (Hz)
TRN
TRN
Control side
Lesioned side

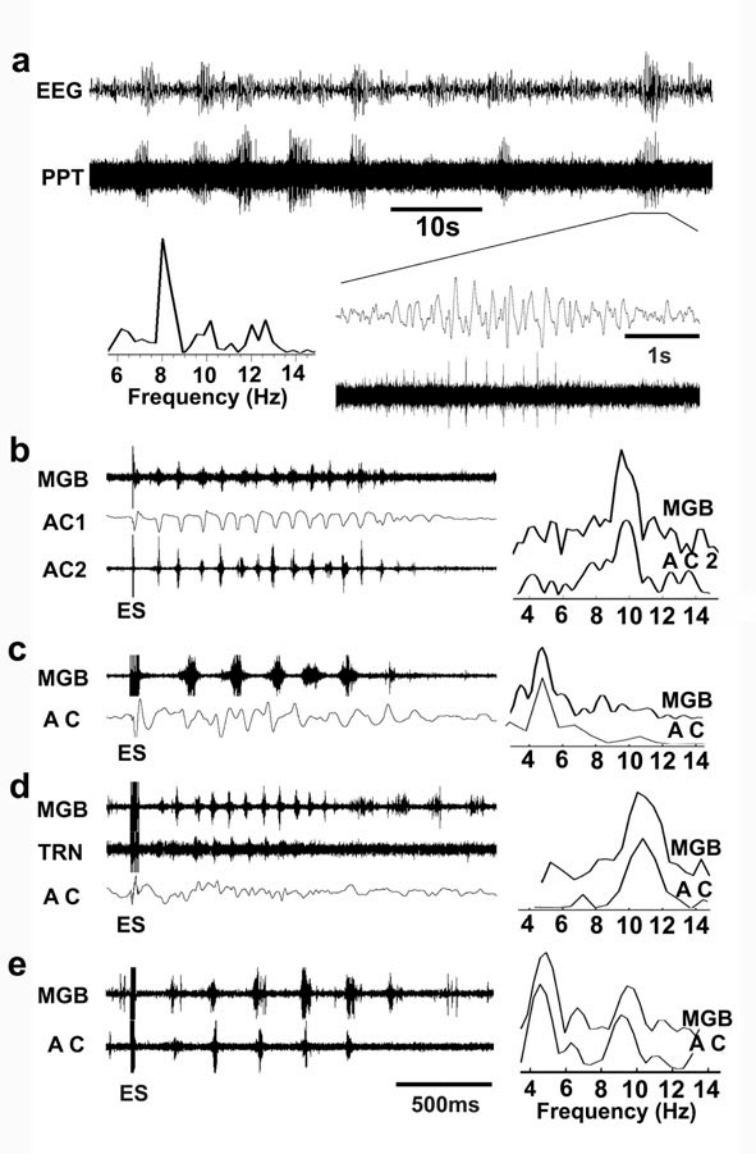
a
EEG
PPT
10s
6 8 10 12 14
Frequency (Hz)
1s
b
MGB
AC1
AC2
ES
MGB
AC2
4 6 8 10 12 14
c
MGB
A C
ES
MGB
A C
4 6 8 10 12 14
d
MGB
TRN
A C
ES
MGB
A C
4 6 8 10 12 14
e
MGB
A C
ES
500ms
MGB
A C
4 6 8 10 12 14
Frequency (Hz)

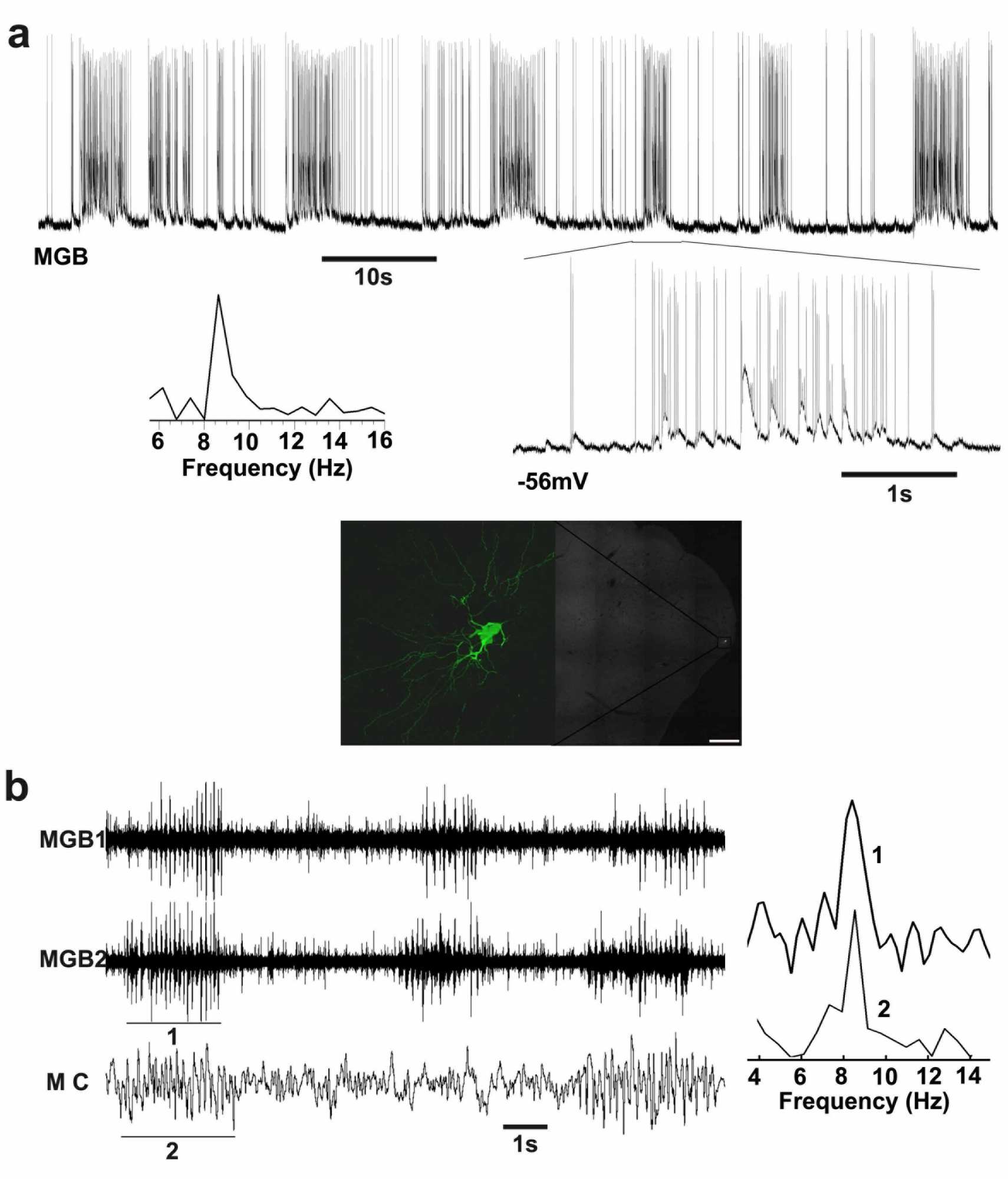
a
MGB
10s
6
8
10
12
14
16
Frequency (Hz)
-56mV
1s
b
MGB1
MGB2
1
M C
2
1s
1
2
4
6
8
10
12
14
Frequency (Hz)